ELSEVIER

Biophysical Chemistry 52 (1994) 145–156

Biophysical Chemistry

An oxygenation-sensitive dye binding to *Carcinus maenas* hemocyanin

Alberto Mazzini [a,*], Mariano Beltramini [b], Roberto Favilla [a], Paolo Cavatorta [a], Paolo Di Muro [b], Benedetto Salvato [b]

[a] *Division of Biophysics and Molecular Biology, Department of Physics, University of Parma, Viale delle Scienze, 43100 Parma, Italy*

[b] *Department of Biology, University of Padova, Padova, Italy*

Received 15 November 1993; accepted 12 May 1994

Abstract

The interaction of 4′,6-diamidino-2-phenylindole (DAPI) with *Carcinus maenas* hemocyanin has been investigated by steady state fluorescence, dynamic fluorescence and circular dichroism measurements. The dye binds to apohemocyanin (without copper) as well as to oxygenated hemocyanin and to deoxygenated hemocyanin with very similar affinities ($k_d \simeq 1$ μM) and number of binding sites (one per subunit). In contrast, the fluorescence quantum yield enhancement of DAPI bound to oxygenated hemocyanin is nearly 60% lower than that observed for deoxygenated and apo forms. The decrease of fluorescence of the dye bound to deoxygenated hemocyanin is a sigmoidal function of the oxygen partial pressure, specular to that observed by following the absorbance of the copper–oxygen charge transfer band at 340 nm. This result provides preliminary evidence that DAPI may be used as a functional probe to monitor the cooperative binding of oxygen to the protein. The higher fluorescence quantum yield of DAPI bound to either apohemocyanin or deoxygenated protein is characterized by a single fluorescence decay with lifetime of about 3 ns, while with the oxygenated protein two components of about 1 ns and 3.0 ns are observed. This result is interpreted assuming the existence of two rotamers of DAPI in solution (Szabo et al. Photochem. Photobiol. 44 (1986) 143–150) both able to interact with oxygenated hemocyanin but only one to deoxygenated and apo forms. We conclude that the different fluorescence behaviour of the dye induced by the presence of oxygen bound to the protein is probably due to a structural change of hemocyanin in cooperative interaction with oxygen. Furthermore, the interaction is confirmed by the induced negative ellipticity of DAPI bound to apohemocyanin and deoxy-hemocyanin and by the increase of fluorescence anisotropy of DAPI bound to all forms of protein investigated.

Keywords: Hemocyanin ; 4′,6-diamidino-2-phenylindole (DAPI); Fluorescence; Binding

1. Introduction

Hemocyanin (Hc) is an oxygen-carrying protein freely dissolved in the hemolymph of several species of *Mollusca* and *Arthropoda* [1]. Its quaternary structure is very different in the two *Phila*: molluscan Hc is a cylindrical molecule composed by a large number of 11S subunits; whereas arthropod Hc is either a single hexamer (16S) arranged as a trigonal antiprism, or an oligohexamer (2×16S; 4×16S; 8×16S), built from a subunit (5S) of about 75000 dalton [1,2]. In both cases the active site contains a couple of copper ions

Abbreviations: DAPI: 4′,6-diamidino-2-phenylindole; apo-Hc: hemocyanin deprived of copper; oxy-Hc: Hemocyanin saturated with oxygen; deoxy-Hc: deoxygenated hemocyanin

* Corresponding author.

SSDI 0301-4622(94)00091-W

directly linked to the protein. In deoxy-Hc the metal is present in the Cu(I) state, while the reaction with oxygen, with a two electron transfer from copper to oxygen, leads to a peroxyde dianion bridge between Cu(II) ions [3]. Dioxygen is bound as a $\mu-\eta^2:\eta^2$ peroxo bridge [4] with concomitant changes in Cu–Cu and N–Cu distances [5,6].

X-ray crystallography data on *Panulirus interruptus* deoxy-Hc at pH 4.5, after crystallization at pH 3.8, have shown that the metal binding site is located in a hydrophobic pocket of the protein matrix. In deoxy-Hc, the metal coordination involves a system of four histidine residues almost coplanar with the two Cu(I) ions (Cu_A, Cu_B); the Cu–N and the Cu_A–Cu_B distances are 0.19 and 0.36 nm respectively and the N–Cu–N bond angle is $\simeq 108°$. Each metal ion is coordinated by a further imidazole nitrogen oriented axially with respect to the ideal plane containing the metal ions and located at a larger bond distance (~ 0.27 nm), the N_{axial}–Cu_A having opposite orientation with respect to N_{axial}–Cu_B [7].

Large contact areas between the subunits stabilizing the hexamer are tighter and better conserved in evolution when they refer to two subunits belonging to two different layers of the trigonal antiprism. Moreover, three large cavities occur within each subunit and two of them are accessible from the solvent: it has been proposed that these cavities may facilitate the penetration of exogenous molecules, including dioxygen, to the active site [7].

The presence of a solvent tunnel extending from the protein surface to the dinuclear copper site completely buried in the protein core results also from the X-ray cristallography model of *Limulus polyphemus* deoxy-Hc. In this case (subunit II, measurements at pH 6.5–7.0) the putative access channel to Cu_A and Cu_B appears to be formed by a cluster of charged residues, conserved in all arthropod Hc sequences and filled with water molecules. Each copper ion has an approximately trigonal planar coordination with angles of 99–131° (N–Cu_A–N) or 97–142° (N–Cu_B–N), ligand-to-metal distances of 0.19–0.22 nm for both metals and Cu_A–Cu_B distances of 0.46 nm [8].

Although the molecular structure of Hc has been the object of several studies and the allosteric behaviour of the protein has been analyzed in great detail (for reviews, see [1–3]), little is known about the structural changes associated with cooperative oxygen binding at a level above the first coordination sphere of the metal. Some investigations in solution have recently been made by using the dye binding method with bromthymol blue (bound to *Limulus polyphemus* Hc) [9] and neutral red (bound to *Panulirus japonicus* Hc) [10]. These indicators are able to monitor the protein structural changes occuring during oxygenation, as evidentiated by little changes in their absorption spectra.

In this perspective we have examinated the binding of the dye 4′,6-diamidino-2-phenylindole (DAPI) (Fig. 1), a well known probe for double stranded nucleic acids [11–14], to *Carcinus maenas* Hc, by exploiting the large enhancement of fluorescence quantum yield observed when this molecule interacts with the protein. This interaction adds to those previously described by us and confirms the dye is able to interact with several proteins [15], beyond phospholipid vesicles and micelles [16].

Here we report on fluorescence studies of the interaction of DAPI with Hc from the mediterranean crab *Carcinus maenas* in three different states: without copper (apo-Hc) and with copper both in air (oxy-Hc) and nitrogen atmosphere (deoxy-Hc). Because of the favourable stoichiometry of binding and different spectroscopic behaviour when bound to oxy- and deoxy-hemocyanin, DAPI appears to be a useful functional probe to study the cooperative oxygenation of this protein.

2. Materials and methods

4′,6-diamidino-2-phenylindole (DAPI.2-HCl) was purchased from Serva and used without further purification and its concentration was spectrophotometrically checked using the absorbance at 344 nm ($\varepsilon_{344} = 23030\ M^{-1}\ cm^{-1}$ [15]). Hemocyanin was extracted from *Carcinus maenas* and purified by following a standard procedure [17]; protein concentration was determined spectrophotometrically using

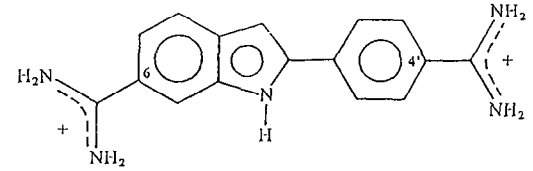

Fig. 1. Chemical structure of 4′,6-diamidino-2-phenyl-indole (DAPI).

$\varepsilon_{278} = 93000\ M^{-1}\ cm^{-1}$ [18], whereas Apo-Hc was prepared by repeated dialysis of the native protein against a solution of CN^- to remove copper [18].

The procedure used to obtain deoxy-Hc was as follows: a solution of oxy-Hc was placed in a tonometer (modified Thunberg tube with the lower part sealed to a fluorescence cuvette [19]), and flushed for ≃45 min with nitrogen gas previously washed and water saturated by bubbling through 10 mM phosphate buffer solution pH = 7.0, and finally discharged in a water trap. The degree of oxygenation was tested by monitoring the intensity of the copper-peroxide charge transfer band at 340 nm ($\varepsilon \simeq 20000\ M^{-1}cm^{-1}$) in the absorption spectrum of the protein and taking the absorbance ratio $A_{340}/A_{278} = 0.21$ for a solution of oxy-Hc.

Mono and bi-sodium phosphate salts were from Merck or C. Erba. All solutions were prepared using water from a Milli-RO plus Milli-Q purification system and the absorbance measurements were done on a Jasco 7850 spectophotometer.

2.1. Fluorescence titrations

All titrations were carried out in 10 mM phosphate buffer pH 7.0, 20°C with a Perkin-Elmer LS50 spectrofluorimeter, equipped with a termostatable cell holder.

Two types of titrations were performed on oxy-Hc, deoxy-Hc and apo-Hc

Type I: at constant dye concentration (~1.5 μM) and variable protein concentration (from ~1 to ~45 μM) to determine ΔF^{I}_{max} values, from double reciprocal plots, hence quantum yields of DAPI bound. The saturation degree of DAPI bound is defined as:

$$\alpha = \frac{[L]_{bound}}{[L]_{tot}} = \frac{\Delta F}{\Delta F^{I}_{max}}$$

and the corresponding Scatchard-like plots (α/P_{free} versus α) were analyzed to determine k_d for the highest affinity sites [20];

Type II: at constant protein concentration (~1.5 μM) and variable dye concentration (from ~1 to ~30 μM) to determine, from the double reciprocal plots, $\Delta F^{II}_{max} = n\Delta F^{I}_{max}$. In this case we have obtained the saturation degree ν by using the normalized ΔF^{I}_{max} as follows:

$$\nu = \frac{[L]_{bound}}{[P]_{tot}} = \frac{\Delta F}{\Delta F^{I}_{max}} \frac{[L]^{I}_{tot}}{[P]^{II}_{tot}}$$

where $[L]^{I}_{tot}$ and $[P]^{II}_{tot}$ are the concentrations of ligand and protein in the two titrations. Then, from the slopes and intercepts of Scatchard plots (ν/L_{free} versus ν) the number of binding sites n and relative affinities were extrapolated and the fluorescence of DAPI free, as deduced from a calibration curve of fluorescence versus concentration of dye, was subtracted from the titration data [20].

In all experiments the protein concentration used was refered to single subunit of 75 kD (5S) and the excitation wavelength was 380 nm, in order to minimize inner filter effects due to absorbances of both dye and protein. Nevertheless, the areas of fluorescence emission peaks were corrected with the reduced Parker's formula [21]:

$$F_{cor} = F_{obs} \frac{2.303\,A}{1 - 10^{-A}}$$

where A was the absorbance of the solution at the excitation wavelength, F_{cor} the corrected fluorescence value and F_{obs} the actual reading. Further correction was done, when necessary, to account for the observed absorbance shift of bound DAPI.

For titrations of deoxygenated protein both Hc and DAPI solutions were fluxed with nitrogen gas and addidions of either deoxy-Hc (type I titration) or DAPI (type II titration) were made with an air-tight syringe.

2.2. Fluorescence anisotropy

Static fluorescence anisotropy data were collected at 450 nm emission wavelength with excitation at 350 nm, according to:

$$A = \frac{I_{vv} - I_{vh}G}{I_{vv} + 2I_{vh}G}$$

where $G = I_{hv}/I_{hh}$. All measurement were performed, at 20°, with the instrument above described.

2.3. Dynamic fluorescence

Time-resolved measurements were made with a single photon counting apparatus equipped with a nitrogen flash lamp (199F Edimburgh Instruments) pulsed at

20 kHz, a stop photomultiplier (Philips XP2020 Q) and fast NIM electronics (Ortec, Silena, Tennelec).

The time resolution was routinely 53 ps per channel and the decays were recorded in a 1024 channel memory. The instrumental response function was automatically collected, in alternation with fluorescence decay, by measuring the scattering of a glycogen solution, and the automatic sampling of the data was driven by a microcomputer. The fluorescence intensity decay data were analyzed as a sum of several exponentials using a global analysis procedure [22]. Samples were prepared with a large excess of hemocyanin ([DAPI] $\simeq 6$ μM; [Hc] $\simeq 44$ μM) and measurements were carried out in a stoppered termostated cuvette ($T = 20$°C), preliminarly fluxed with nitrogen gas in the case of deoxy-Hc, as described before.

2.4. Circular dichroism

CD measurements were carried out, at constant temperature (20°C) with a Jasco dichrograph J500, at high concentrations of both dye and protein (~ 35 μM each), in order to obtain a fairly good saturation (about 85% of DAPI bound to the protein assuming $k_d \simeq 1$ μM and one site per subunit) together with an appropriate absorbance of DAPI (OD $\simeq 0.8$ in 1.0 cm cell at 345 nm). The actual reading gives a direct measure of ellipticity θ (deg) according to

$$\theta = \frac{2.303(A_L - A_R)180}{4\pi},$$

where A_L and A_R are the absorbances of left and right circularly polarized light, respectively. This parameter (θ) allows us to compare our results, since the same molar concentration of DAPI was used troughout in our CD measurements.

2.5. Oxygen equilibrium measurements

The oxygen binding curve of Hc was determined according to standard tonometric methods with concomitant determination of the saturation fraction by means of different optical signals: in the case of Hc alone we have followed the absorbance intensity of the 340 nm band of oxy-Hc ($\varepsilon = 20000\ M^{-1}\,cm^{-1}$) or the quenching of the tryptophan emission band at 355 nm (excitation wavelength 295 nm), resulting from oxygen binding and previously demonstrated to be linearly correlated with the degree of oxygenation [23]. In the case of Hc (1.5 μM) plus DAPI (5.0 μM) we have followed both the absorption at 340 nm of oxy-Hc, as above, and the quenching of DAPI emission at 440 nm (excitation wavelength 390 nm).

The solutions were previously equilibrated in a tonometer with a water-saturated N_2 atmosphere at 20°C and, then, titrated with aliquots of water-saturated O_2 added by means of an air tight syringe. The final $p(O_2)$ is calculated as:

$$p(O_2) = \frac{v}{V}(760 - 17.5),$$

where v and V are the volumes (ml) of added O_2 and tonometer respectively. The gas pressure inside the tonometer is kept equal to the atmospheric pressure (760 mm Hg) and corrected for the 17.5 mm Hg, the water partial pressure at 20°C [24]. No corrections have been made for barometric pressure.

3. Results

DAPI interacts at pH 7.0 with oxy-, deoxy- and apo-Hcs and the large spectral shifts observed, as a consequence of this interaction, are similar to those observed for the case of binding with poly d(G-C) [25] and other systems [14]. The interaction with Hc is accompained by a small red-shift ($\simeq 5$ nm) and a small hypochromicity (10%) in the absorbance spectrum of DAPI, whereas a large blue-shift ($\simeq 25$ nm for apo-Hc and deoxy-Hc, $\simeq 20$ nm for oxy-Hc) and a very large emission enhancement (from 10 to 25 times) are observed in the fluorecence spectrum of the dye. Fig. 2 shows typical absorbance and emission spectra of free DAPI and of DAPI bound to apo-Hc. An example of fluorescence titration relative to DAPI binding to apo-Hc is shown in Fig. 3.

Upon binding to all protein forms, the static anisotropy of fluorescence, measured using $\lambda_{ex} = 380$ nm and $\lambda_{em} = 430$ nm, increases from 0.1 (DAPI alone) to 0.34 (DAPI bound).

The integrated fluorescence signals were used to analyze the interaction of the dye with apo-Hc, deoxy-Hc and oxy-Hc (Figs. 4, 5 and 6 respectively) in terms of double reciprocal (Fig. 4a, 5a and 6a) and Scatchard-like plots (Figs. 4b, 5b and 6b) for type I titrations, and of double reciprocal (Figs. 4c, 5c, and 6c) and

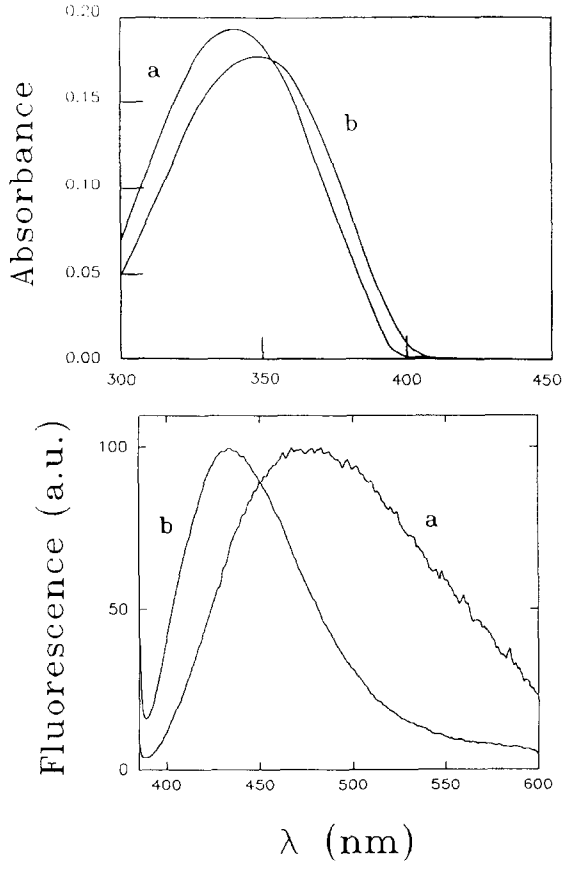

Fig. 2. Absorbance and fluorescence spectra of DAPI free and bound to apo-Hc. Upper panel: absorbance spectra; lower panel: normalized and corrected fluorescence emission spectra ($\lambda_{ex} = 380$ nm) of 1.44 μM DAPI alone (a) and with 34.4 μM apo-Hc (b), 10 mM phosphate buffer pH 7.0, 20°C.

Scatchard plots (Figs. 4d, 5d and 6d) for type II titrations (see Ref. [20] for complete analysis of fluorescence binding data). The values of the dissociation constants (k_d), number of binding sites per subunit (n) and enhancement of fluorescence quantum yield (Q) obtained from these experiments are sumarized in Table 1.

The fluorescence emission spectrum of DAPI in the presence of oxygenated protein is about 60% lower and shows a maximum 5 nm red-shifted as compared to that observed for apo-Hc or deoxy-Hc, while the emission spectrum of DAPI alone does not show any intensity variation after treatment with oxygen or nitrogen gas. This fluorescence quenching by oxygen is completely reversible: the emission spectrum of the DAPI bound to the protein increases under nitrogen atmosphere and decreases again to the original value when the protein is again saturated with oxygen (Fig. 7, upper panel). In agreement, the fluorescence intensities recorded by titrating deoxy-Hc with DAPI are higher than those obtained with oxy-Hc (Fig 7, lower panel curves b and a respectively). When deoxy-Hc is saturated again with oxygen, its DAPI titration curve is almost superimposable to that of an oxy-Hc sample (Fig. 7, lower panel, curve c). In these titrations no appreciable differences of affinity or number of binding sites are observed.

Since the oxygenation of hemocyanin induces an appreciable quenching of the fluorescence of bound DAPI, we have determined the oxygen binding curve of deoxy-Hc in experiments carried out at constant DAPI concentration and variable partial pressure of oxygen. The results are compared with those for Hc in the absence of dye: the p_{50} (partial pressure in mm Hg corresponding to half saturation of the protein) and

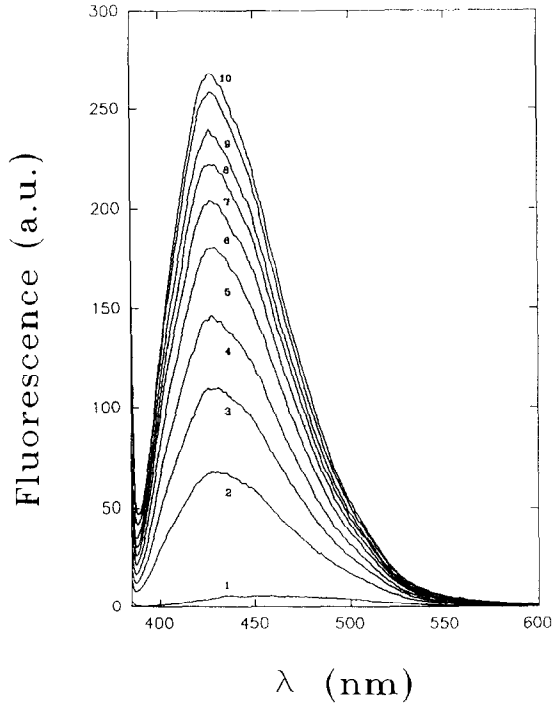

Fig. 3. Fluorescence titration of apo-Hc with DAPI. Uncorrected emission fluorescence spectra of 1.4 μM DAPI alone (1) and in the presence of increasing concentrations of apo-Hc from 1 to 34 μM (2 → 10). Other conditions as in Fig. 2.

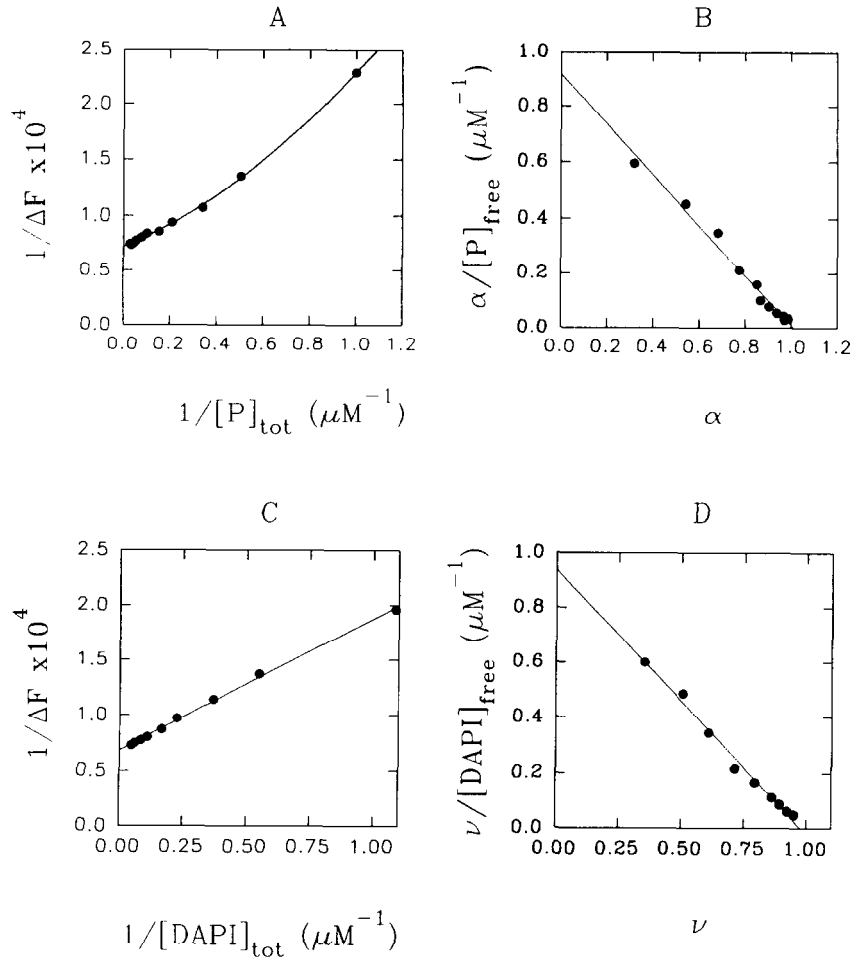

Fig. 4. Titration with apo-Hc. (A): Double reciprocal plot and (B): Scatchard-like plot relative to type I titration; [DAPI] = 1.44 μM, [apo-Hc] from 1 to 34.2 μM; $\Delta F^{I}_{max} = 13600$. (C): Double reciprocal plot and (D): Scatchard plot relative to type II titration; [apo-Hc] = 1.52 μM, [DAPI] from 0.9 to 21.2 μM; $\Delta F^{II}_{max} = 14420$. (For definition of α and ν see Section 2). Other conditions as in Fig. 2.

h_{max} (maximum slope in the Hill plot), relative to oxygen binding to Hc at pH 7.0, are 64.3 mmHg and 2.8 in the absence of DAPI and 65.3 mmHg and 2.6 in the presence of 5 μM DAPI (Hc = 1.5 μM), respectively.

At the concentration used, therefore, the binding of DAPI to Hc (up to a 77% saturation) does not affect the binding of O_2. Furthermore, the quenching of the emission of bound DAPI is linearly correlated with the degree of saturation of the protein, similarly to the effect observed on tryptophan emission [23]. As a consequence, a straight line with slope 1 is obtained by plotting the oxygen fractional saturation of the protein in absence of DAPI (as monitored at the 340 nm absorption band) versus the fractional saturation of the Hc-DAPI adduct (as monitored by the quenching of 440 nm DAPI emission (Fig. 8)).

The fluorescence decay of free and bound DAPI to various forms of Hc is characterized by the values of lifetime (τ), normalized pre-exponential factors (α) and fractional contributions to the fluorescence of each decay component (F) reported in Table 2. A typical fluorescence decay of DAPI bound to oxy-HC is shown in Fig. 9. These parameters, obtained with $\lambda_{ex} = 350$ nm and $\lambda_{em} = 440$ nm, are deduced from a global analysis considering several emission wavelengths from 400 to 500 nm.

As deduced from χ^2 values and randomness of residuals, the decay curves relative to DAPI complexed with

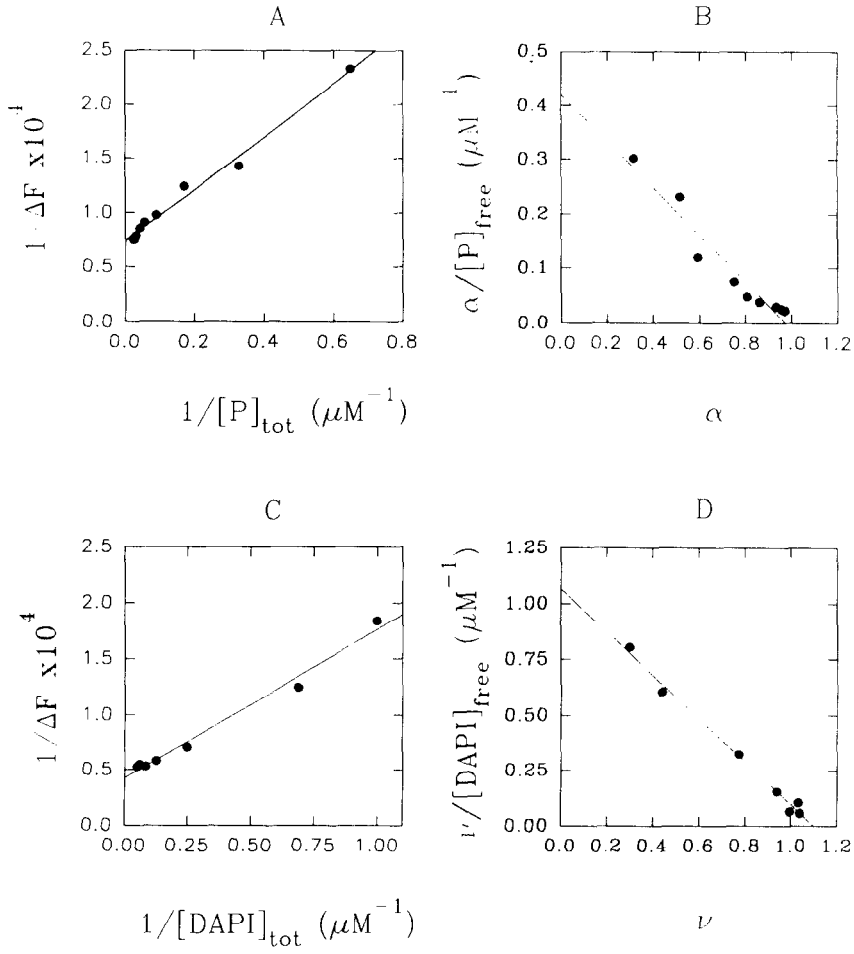

Fig. 5. Titration with deoxy-Hc. (A): Double reciprocal plot and (B): Scatchard-like plot relative to type I titration; [DAPI] = 1.57 μM, [deoxy-Hc] from 1.54 to 43.2 μM; $\Delta F^{I}_{max} = 13570$. (C): Double reciprocal plot and (D): Scatchard plot relative to type II titration; [deoxy-Hc] = 2.1 μM, [DAPI] from 1.0 to 20.0 μM; $\Delta F^{II}_{max} = 19800$. The solution of DAPI and protein were fluxed with nitrogen gas for ~45 minutes before starting the measure. (For definition of α and ν see Section 2.) Other conditions as in Fig. 2.

deoxy-Hc and apo-Hc are well fitted by a single exponential, while two exponential decays are observed for the case of DAPI bound to oxy-Hc.

The near-UV-CD spectrum of DAPI bound to apo-Hc, shown in Fig. 10, shows a profile with a maximum of negative ellipticity at about 350 nm (similar results are obtained with deoxy-Hc). The CD spectrum of DAPI bound to oxy-Hc is completely overlapped with the strong negative band of the protein at 335 nm [26], but its intensity is slightly higher than that for the protein alone (data not shown).

4. Discussion

The dye 4′,6-diamidino-2-phenylindole belongs to the family of fluorescent probes whose emissive properties are markedly affected by the interactions with macromolecules or supramolecular aggregates like phospholipid vesicles and micelles [15,16]. In this paper we have studied the interaction of DAPI with Hc that, given its oligomeric structure, may exhibit different binding sites for the dye either at the subunit interfaces or within a subunit. Furthermore, the protein can

be studied at least in three forms, namely oxy-Hc, deoxy-Hc and apo or copper deprived form, thus enabling one to disclose possible differences in binding capacity as a function of the active site state and/or conformational changes associated with the binding of oxygen itself. The binding of DAPI to either Hc form is characterized by the same dissociation constant and number of sites per subunit, as well as by a blue-shift and intensity enhancement of the emission spectrum, an increase of fluorescence polarization, changes of pre-exponential factors and lifetime values in the emission decay curve and presence of negative ellipticity in the absorption band near 345 nm.

Table 1
Binding parameters k_d, n and Q (fluorescence enhancement factor) relative to the interaction of DAPI at 20°C with apo-HC, oxy-HC and deoxy-HC

	k_d (μM) [a]	n [b]	Q
apo-HC	1.0	1.0	23
deoxy-HC	0.9	1.1	25
oxy-HC	0.9	1.0	10

[a] The standard deviations of the dissociation constants, calculated from a set of at least three measures for each protein form, were lower than 20%.
[b] n is referred to the single subunit of 75 kD molecular weigth.

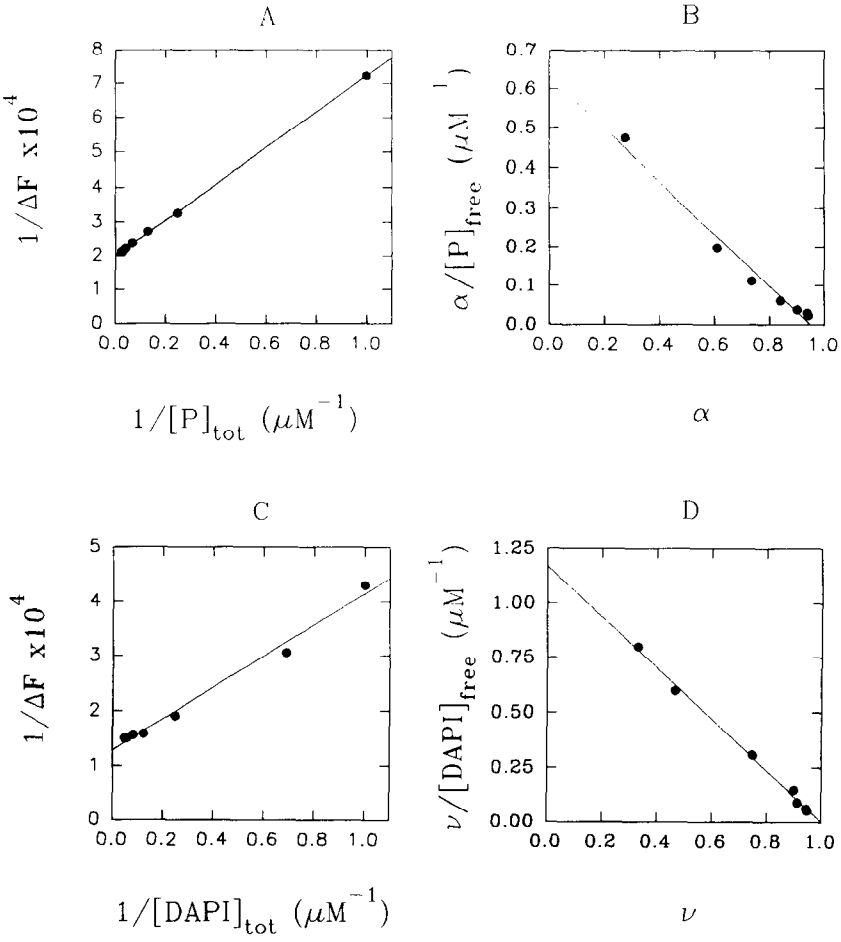

Fig. 6. Titration with oxy-Hc. (A): Double reciprocal plot and (B): Scatchard-like plot relative to type I titration; [DAPI] = 1.44 μM, [oxy-Hc] from 1 to 41.3. μM; $\Delta F^{I}_{max} = 5000$ (C): Double reciprocal plot and (D): Scatchard plot relative to II titration; [oxy-Hc] = 2.1 μM, [DAPI] from 1 to 20 μM; $\Delta F^{II}_{max} = 7700$. (For definition of α and ν see Section 2. Other conditions as in Fig. 2.

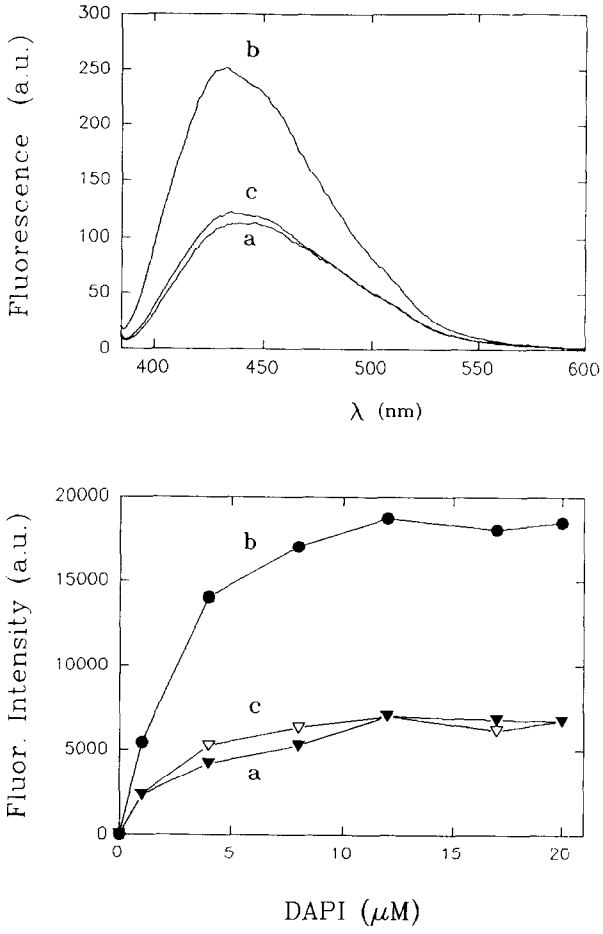

Fig. 7. Oxygen effect on the fluorescence of DAPI bound to hemocyanin. Upper panel: emission fluorescence spectra of DAPI bound to deoxy-Hc and oxy-Hc ([Hemocyanin] = 2 μM, [DAPI] = 17 μM). (a): oxy-Hc; (b): deoxy-Hc (sample (a) after 45 min of nitrogen flux); (c): oxy-Hc (sample (b) exposed again to air for 45 min). Lower panel: areas of fluorescence emission spectra of DAPI bound, subtracted by areas of fluorescence emission spectra of DAPI free at the relative different concentrations. [Hemocyanin] = 1.5 μM, [DAPI] = from 1.5 to 37 μM. Other conditions as in Fig. 2.

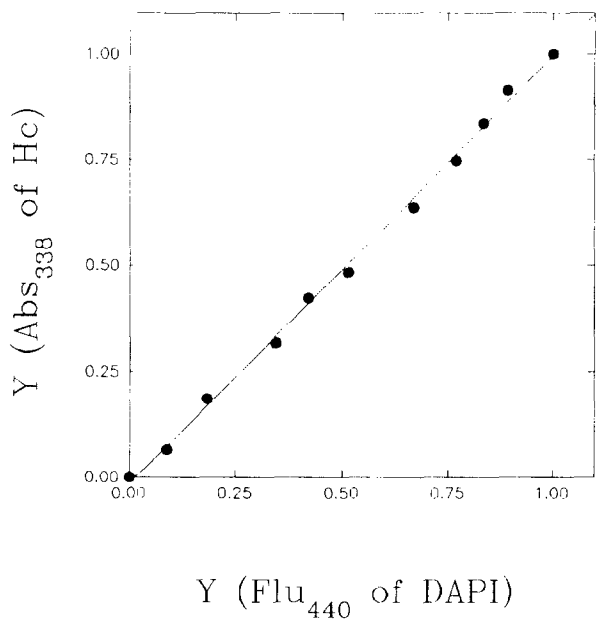

Fig. 8. Oxygen saturation (Y) with and without DAPI bound. The oxygen saturation Y was calculated from the absorbance at 338 nm of Hc in the absence of DAPI (y axis) and comparated to that from the emission fluorescence quenching (x axis) of DAPI bound to the protein ($\lambda_{ex} = 390$ nm, $\lambda_{em} = 440$ nm). [Hc] = 1.5 μM; [DAPI] = 5 μM.

The different fluorescence intensity of DAPI bound to different forms of hemocyanin may suggest alternative interpretations: (a) a direct paramagnetic quenching due either to oxygen itself or copper, which changes its oxidation state from +1 to +2 or (b) a change of protein conformation occurring when oxygen binds to hemocyanin.

Considering that a paramagnetic effect implies a close proximity between fluorophor and quencher [27], the first hypothesis would imply the binding sites for DAPI and oxygen to be near each other.

If this were the case the interaction with oxygen should be expected to affect the binding strength of the dye molecule. Since this is not observed, we attribute the different fluorescence quantum yield of DAPI bound to oxy-Hc to protein conformational changes.

Table 2
Lifetimes (τ_1, τ_2), normalized pre-exponential factors (α_1, α_2), fractional contributions of each decay component (F_1, F_2) and reduced χ^2 values relative to DAPI free and bound to apo-HC, oxy-HC and deoxy-HC ($\lambda_{ex} = 350$ nm, $\lambda_{em} = 440$ nm, in phosphate buffer 0.01 M pH 7, $T = 20°$). The values are obtained from a global analysis procedure: the lifetimes remain constant over the wavelength range investigated (from 400 to 500 nm)

DAPI with	τ_2 (ns)	τ_1 (ns)	α_2	α_1	F_2	F_1	χ^2
apo-HC	3.0	–	1.0	–	1.0	–	1.5
deoxy-HC	3.0	–	1.0	–	1.0	–	1.6
oxy-HC	3.1	1.0	0.24	0.76	0.49	0.51	1.6
–	2.8	0.2	0.04	0.96	0.44	0.56	1.3

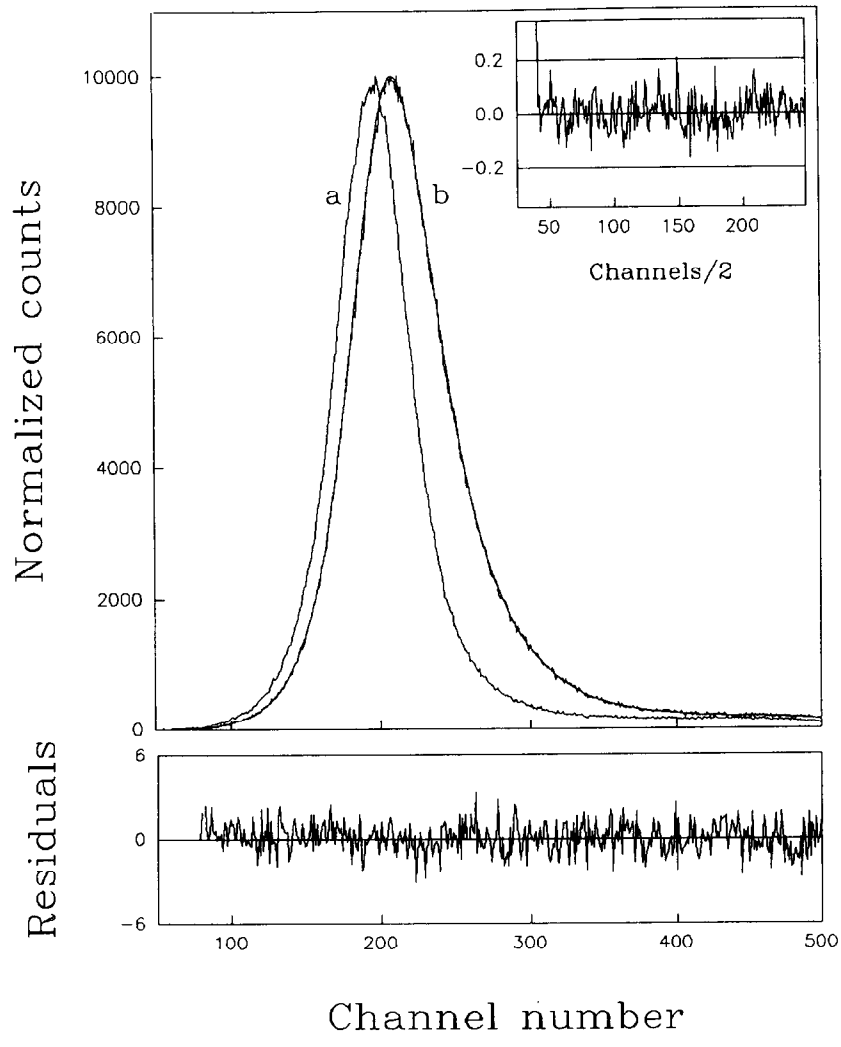

Fig. 9. Fluorescence decay profile of DAPI bound to oxy-Hc. DAPI: 6.9 μM, oxy-Hc: 43.0 μM in phosphate buffer 10 mM, pH 7, at $T = 20°$ ($\lambda_{ex} = 350$ nm; $\lambda_{em} = 440$ nm, channel width = 0.053 ns). The peak (a) is the instrumental response function, the noisy plot (b) is the decay of DAPI bound to oxy-Hc. The superimposed smooth line represents the convoluted fitted function and the lower graph is the plot of weighted residuals, whereas in the upper right corner the autocorrelation of the residual is represented.

In order to examine whether DAPI could be used to monitor partially oxygenated states of hemocyanin, the fluorescence intensity decrease of the dye as a function of oxygen partial pressure of oxygen was measured. The observation that oxygen saturation function is coincident with those obtained by following protein intrinsic probes (such as absorbance of copper-peroxide charge transfer band and fluorescence quenching of tryptophan) suggests also the use of DAPI as a functional probe of hemocyanin.

Since the time-resolved fluorescence of DAPI in solution clearly shows two distinct time components, according to the model of Szabo et al. [28], we assume the existence of two different conformers R1 (with 6-amidinium group planar with the indole ring) and R2 (with the substituent twisted out of the indole plane) (Scheme 1).

The indole ring of the excited conformer in the planar configuration, R1*, becomes more basic and undergoes a rapid proton transfer from the 6-amidinium group,

during the lifetime of the excited singlet state ($\tau_1 \simeq 0.2$ns). Furthermore, the fluorescence of DAPI complexed with either DNA [28], bovine serum albumin [15], or phospholipid vesicles [16] was rationalized, by assuming that the intramolecular proton transfer is inhibited upon binding, thus leading to a decay of about 1 ns from R1*.

This scheme appears to be also valid for the fluorescence behaviour of DAPI bound to Hc. In fact, the fluorescence decay of the DAPI- oxy-Hc complex is well fitted by two exponential components (lifetimes of about 3.0 ns and 1.0 ns), suggesting that both R1 and R2 conformers are involved in the interaction, as in the case of bovine serum albumin ($\tau_2 \simeq 2.8$ ns, $\tau_1 \simeq 1.0$ ns) [15].

However, since only the long lifetime component (about 3.0 ns) is observed for DAPI-deoxy-Hc and DAPI-apo-Hc, only the twisted out of plane conformer R2 can be deduced to interact with these protein forms.

Thus, our findings suggest that DAPI binds to deoxy-Hc and apo-Hc with more stringent structural constraints, the only non-planar R2 rotamer being able to interact with them. This interpretation can be further

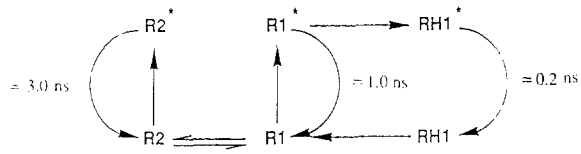

Scheme 1. Proposed model for the fluorescent behaviour of DAPI alone and in complexes with either dsDNA, proteins or phospholipid structures.

supported by the higher fluorescence quantum yield of DAPI-deoxy-Hc and DAPI-apo-Hc complexes, compatible with a selective binding of the long lived R2 rotamer only, as well as by the analysis of the emission spectra of DAPI bound to oxy-Hc and deoxy-Hc which show different maximum wavelengths.

It is likely, therefore, that a protein conformational transition, following oxygen binding, induces a higher exposure of DAPI binding sites, which can accomodate both R1 and R2 rotamers with a concomitant decrease of fluorescence intensity of the dye.

A further confirmation of the binding of DAPI molecules to the various forms of Hc arises from circular dichroism measurements. In fact DAPI, becomes opti-

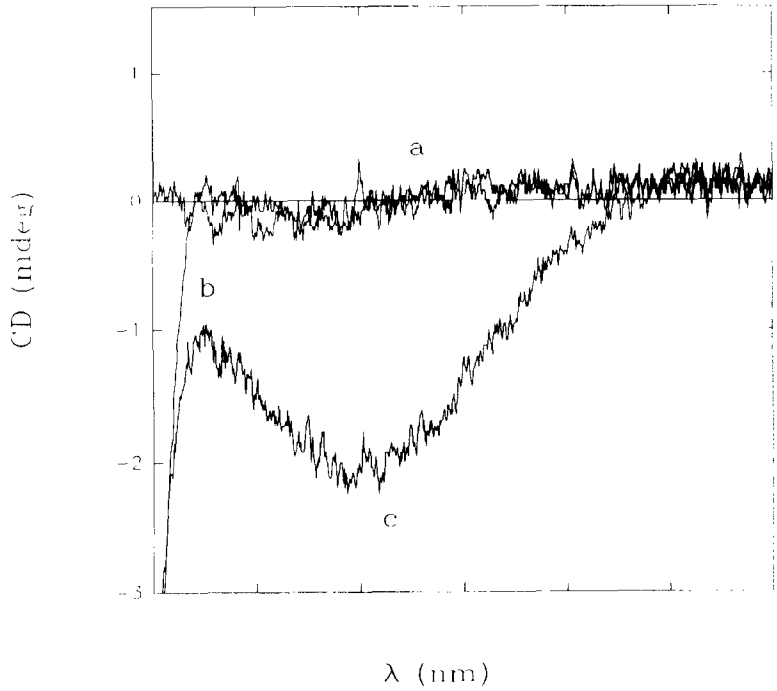

Fig. 10. Circular dichroism spectrum of DAPI bound to apo-Hc. (a) [DAPI] = 37 μM; (b) [Apo-Hc] = 37 μM; (c) [Apo-Hc] = 37 μM plus [DAPI] = 37 μM. Other conditions as in Fig. 2.

cally active (with a negative ellipticity) only upon binding to either Apo-Hc, Deoxy-Hc or oxy-Hc with a similar spectrum in all cases. However, the circular dichroism seems to be less sensitive than the fluorescence technique on monitoring the selective binding of the two dye rotamers to the various forms of protein.

References

[1] B. Salvato and M. Beltramini, Life Chem. Rept. 8 (1990) 1–47.
[2] G. Préaux and C. Gielens, in: Copper proteins and copper enzymes, ed. R. Lontie (CRC Press, Boca Raton, 1984) pp. 159–205.
[3] H.D. Ellerton, N.F. Ellerton and H.A. Robinson, Progr. Biophys. Mol. Biol. 41 (1983) 143–248.
[4] K. Magnus and H. Ton-That, J. Inorg. Biochem. 74 (1992) 24.
[5] M.C. Feiters, Comm. Inorg. Chem. 11 (1990) 131–174.
[6] M.C. Feiters, International Congress on Invertebrate Dioxygen Carriers, Lunteren (The Netherlands), Book of Abstracts IIIL, eds. A. Volbeda and W.G.J. Hol, J. Mol. Biol. 209 (1989) 249–279.
[7] A. Volbeda and W.G.J. Hol, J. Mol. Biol. 209 (1989) 249–279.
[8] B. Hazes, K.A. Magnus, C. Bonaventura, J. Bonaventura, Z. Dauter, K.H. Kalk and W.G.J. Hol, Protein Sci. 2 (1993) 597–619.
[9] N. Makino, Eur. J. Biochem. 146 (1985) 563–569.
[10] N. Makino, Eur. J. Biochem. 163 (1987) 35–41.
[11] W.D. Wilson, F.A. Tanious, H.J. Barton, R.L. Jones, K. Fox, R.L. Wydra and L. Strekowski, Biochemistry 29 (1990) 8452–8461.
[12] M.L. Barcellona and E. Gratton, Eur. Biophys. J. 17 (1990) 315–323.
[13] P. Cavatorta, L. Masotti and A.G. Szabo, Biophys. Chem. 22 (1985) 11–16.
[14] S.K. Kim, S. Eriksson, M. Kubista and B. Nordn, J. Am. Chem. Soc. 115 (1993) 3441–3447.
[15] A. Mazzini, P. Cavatorta, M. Iori, R. Favilla and G. Sartor, Biophys. Chem. 42 (1992) 101–109.
[16] R. Favilla, G. Stecconi, P. Cavatorta, G. Sartor and A. Mazzini, Biophys. Chem. 46 (1993) 217–226.
[17] L. Bubacco, R.S. Magliozzo, M. Beltramini, B. Salvato and J. Peisach, Biochemistry 31 (1992) 9294–9303.
[18] B. Salvato, A. Ghiretti–Magaldi and F. Ghiretti, Biochemistry 13 (1974) 4778–4783.
[19] B. Giardina and G. Amiconi, in: Methods enzymology. Measurements of binding of gaseous and non gaseous ligands to hemoglobin by conventional spectrophotometric procedures (Academic Press, New York, 1981) pp. 417–427.
[20] R. Favilla and A. Mazzini, Biochim. Biophys. Acta 788 (1984) 48–57.
[21] C.A. Parker, Photoluminescence of solutions (Elsevier, Amsterdam, 1968) 220–233.
[22] J.R. Knutson, J.M. Beechem and L. Brand, Chem. Phys. Letters 102 (1983) 501–507.
[23] N. Shaklai and E. Daniel, Biochemistry 9 (1970) 564–568.
[24] R.C. Weast, ed., Handbook of Chemistry and Physics, 54th Ed. (CRC Press, Boca Raton, 1970) p. D-159.
[25] W.D. Wilson, F.A. Tanious, H.J. Barton, L. Strekowski and D.W. Boykin, J. Am. Chem. Soc. 111 (1989) 5008–5010.
[26] M. Beltramini, L. Bubacco, B. Salvato, L. Casella, M. Gullotti and S. Garofani, Biochim. Biophys. Acta 1120 (1992) 24–32.
[27] D.M. Hercules, Methods Enzymol. 11 (1967) 776–856.
[28] A.G. Szabo, D.T. Krajcarski, P. Cavatorta, L. Masotti and M.L. Barcellona, Photochem. Photobiol. 44 (1986) 143–150.